A Novel Matrix Transformation for Decoupled Control of Modular Multiphase PMSM Drives

A Novel Matrix Transformation for Decoupled Control of Modular Multiphase PMSM Drives

Sandro Rubino, *Member, IEEE*, Obrad Dordevic, *Member, IEEE*, Eric Armando, *Senior Member, IEEE*, Radu Bojoi, *Fellow, IEEE*, and Emil Levi, *Fellow, IEEE*

***Abstract*–When multiphase drives are used for specific applications, the modular solutions are preferred as they use consolidated power electronics technologies. The literature reports two modeling approaches for multiphase machines having a modular configuration of the stator winding. The first approach is the vector space decomposition (VSD) that models the energy conversion like an equivalent three-phase machine. The main alternative to the VSD is the multi-stator (MS) modeling that emphasizes machine modularity in terms of torque production. Both approaches have advantages and disadvantages for multiphase machines with a modular structure. Therefore, this paper aims to combine the VSD and MS approaches, defining a new matrix transformation and hence developing a new modeling approach for multiphase machines with a modular structure. The proposed transformation allows a decoupled and independent torque control of the sets composing the machine, preserving the torque regulation's modularity. Together with a new vector control scheme, it has been applied to a modular permanent magnet synchronous machine (PMSM) with a non-standard spatial shift between windings. Experimental results are presented for a nine-phase PMSM prototype with a triple-three-phase stator winding configuration.**

***Index Terms*–Modular vector control, multiphase machines, multi-stator, permanent magnet synchronous motors, vector space decomposition.**

I. INTRODUCTION

Multiphase machines are today a competitive solution in the electrification processes of transport and energy production from renewables [1], [2]. Due to the significant cost reduction of the conventional power electronics technologies, an important development is reported for the multiphase drives using a modular configuration of the stator winding [3], [4]. A further reason for this trend is related to the remarkable know-how that is nowadays available in the literature for the conventional drive topologies, i.e., three-phase [5], five-phase [6]–[8], and six-phase configurations [9]–[11].

According to the literature [2], [12]–[14], most of the control algorithms for multiphase drives are based on the vector space decomposition (VSD) approach [15], [16]. The VSD decomposes the machine model into multiple orthogonal subspaces using a dedicated VSD matrix transformation. The energy conversion is performed in a single subspace, having the meaning of the machine's time-fundamental model, characterized by electromagnetic equations similar to those of the three-phase motors. The other subspaces have the meaning of the machine's harmonic patterns, highlighting possible unbalance among the stator phases in terms of currents, fluxes, and torque [17], [18].

The VSD transformation matrix exists for multiphase machines with the stator winding in either symmetrical or asymmetrical configuration [16], [19], thus covering most practical cases. Besides, since the VSD modeling allows using all the control algorithms defined for three-phase motor drives, it results in the literature's most developed approach [13], [14]. Therefore, significant efforts have been made in the development of VSD-based pulse-width modulation (PWM) techniques [19], using both space-vector (SV) [20]–[22] and carrier-based (CB) methods [23], [24]. Lastly, almost all of the open-phase fault-tolerant strategies are based on the active control of the harmonic VSD subspaces [14], [25]–[28].

Nevertheless, the VSD approach exhibits several limitations in modeling multiphase machines having a modular configuration of the stator winding. The first limitation is the lack of modularity [16], as the VSD does not emphasize the torque production of each winding set composing the stator. The second limitation is the applicability to only machines with conventional symmetrical/asymmetrical stator configurations [29]. Finally, the modular configurations are usually adopted when the number of phases is high ($\geq$ 6), making the implementation of VSD-based PWM techniques more challenging [19]. This issue worsens if an open-phase fault occurs, as the post-fault operation often requires the whole redefinition of the PWM space-vector algorithms [30].

The drawbacks of the VSD in dealing with the modular configurations can be solved with the multi-stator (MS) modeling [1], [31]. This approach models the machine as multiple winding sets operating in parallel. Each of these must consist of an l-phase configuration ($l \geq 3$), having an isolated neutral point treated with a dedicated VSD transformation [29]. In this way, the torque production of each set is highlighted through its own time-fundamental VSD subspace. An example is represented by the multi-three-phase machines [1], [3], [4], [32], where the stator consists of multiple three-phase winding sets, allowing the use of the three-phase Clarke transformation (the simplest VSD case for l=3). Therefore, if a machine having n winding sets is considered, n time-fundamental VSD subspaces are obtained [33]–[35]. Each of the latter highlights the torque produced by the windings set of which it is representative.

Manuscript received July 17, 2020; revised October 22, 2020; accepted November 24, 2020.

Sandro Rubino, Eric Armando and Radu Bojoi are with the Dipartimento Energia "G. Ferraris", Politecnico di Torino, Torino, 10129, Italy (e-mail: sandro.rubino@polito.it; eric.armando@polito.it; radu.bojoi@polito.it).

Obrad Dordevic and Emil Levi are with the Faculty of Engineering and Technology, Liverpool John Moores University, Liverpool L3 3AF, U.K., (e-mail: o.dordevic@ljmu.ac.uk; e.levi@ljmu.ac.uk).

In summary, MS modeling can be considered as a modular application of the VSD approach to multiphase machines. In this way, the VSD constraints in terms of symmetrical and asymmetrical configurations are restricted to the single *l*-phase winding set. Besides, an MS-based control scheme allows implementing modular PWM algorithms, as the voltage control of each winding set is independent of that of the others [33]. However, MS modeling leads to strong magnetic coupling among the winding sets [33], [34], [36], [37]. As demonstrated in [38], this effect can cause the potential instability of the MS-based control schemes, making necessary the implementation of complex decoupling algorithms [33], [34], [36], [37].

In recent years, several attempts to combine the advantages of VSD and MS modeling approaches have been suggested [39], [40], and most of them are focused on removing the MS couplings among the winding sets. According to the literature, this goal has been successfully reached in [41], where a decoupling transformation for a dual-three-phase permanent magnet synchronous motor (PMSM) was introduced, leading to a decoupled MS-based current vector control (CVC) scheme. In [42], a decoupling transformation for multi-three-phase induction machines (IMs) has been presented, allowing the implementation of a modular torque control scheme. However, it appears that no solutions that can extend the results obtained in [41], [42] to a generic modular multiphase configuration for PMSMs are available in the literature.

Therefore, the goal of this paper is to develop a novel matrix transformation for removing the MS couplings of a multiphase PMSM, allowing the implementation of a modular and decoupled CVC scheme. The proposed solution can be applied to any modular multiphase configuration, thus assuming general validity. The contributions of this paper are:

1) a new modeling approach for multiphase PMSMs having a modular configuration of the stator winding;
2) an original CVC scheme able to perform a decoupled regulation of the torque produced by each winding set.

Compared to the existing VSD-based control schemes, the advantages of the devised control solution are:

- direct regulation of the currents belonging to each winding set, thus keeping control modularity;
- possibility of controlling any modular multiphase PMSM, including the machines with stator windings that are neither symmetrical nor asymmetrical [29];
- the torque-sharing strategies among the winding sets can be implemented using their time-fundamental models, avoiding the active control of the harmonic VSD subspaces [17];
- each winding set is fed by its *l*-phase voltage source inverter (VSI), controlled by any of the VSD-based PWM techniques reported in the literature [19].

The proposed CVC scheme, along with the novel transformation matrix, further results in the following benefits:

- the MS couplings among the winding sets are removed, avoiding the need to implement decoupling algorithms whose performance depends on the accuracy of the machine parameter estimation [33], [34];

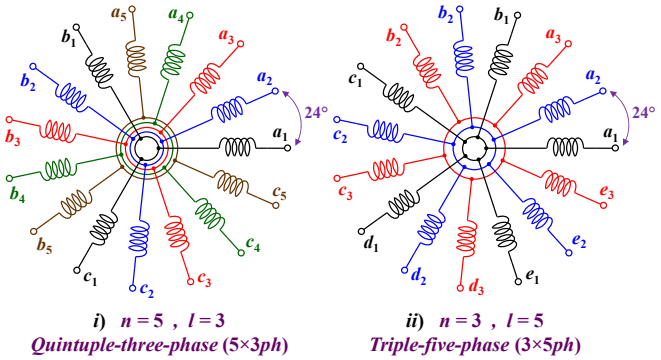

i) $n = 5$, $l = 3$ *Quintuple-three-phase* (5×3*ph*)

ii) $n = 3$, $l = 5$ *Triple-five-phase* (3×5*ph*)

Fig. 1. Examples of multiphase windings with a modular configuration.

- each winding set's torque is controlled using common- and differential-mode variables, leading to a decoupled regulation scheme, as for a VSD-based control algorithm.

Finally, thanks to the combination of both VSD and MS modeling approaches, the introduced CVC scheme allows the implementation of two different fault-tolerant strategies:

- fault ride-through capability of the winding sets, as for each of these the VSD-based fault strategies reported in the literature (open-phase-fault) can be applied [14];
- the machine's modular fault ride-through capability, since in the case of an open-phase fault, the affected winding set can be entirely turned off [1].

The experimental validation of the proposed modeling approach and related CVC scheme has been carried out on a 9-phase PMSM prototype that uses a triple-three-phase configuration of the stator winding.

The paper is organized as follows. Section II describes the modeling approach, introducing the new decoupling transformation. The modular and decoupled CVC scheme is presented in Section III, while the experimental validation is reported in Section IV. Lastly, Section V provides conclusions.

II. Modular and Decoupled Modeling Approach

In the following, a multiphase PMSM having a modular configuration of the stator winding is considered. The following conditions are assumed:

- the stator consists of an arbitrary number n of l-phase winding sets ($l \geq 3$), each of them having its own and isolated neutral point;
- the winding sets are equal one to the other, thus having the same values of resistance R_s, leakage inductance $L_{\sigma s}$, and number of winding turns;
- the winding sets have a symmetrical or asymmetrical configuration, allowing the application of a dedicated VSD transformation to each of them [29];
- the windings are sinusoidally distributed, interacting with each other and the permanent magnets (PM) only through the spatial-fundamental component of the airgap field;
- magnetic saturation, iron losses, and mutual leakage couplings among the phases are not considered.

No constraints on the number of pole-pairs p and magnetic phase-shift among the first phases of two consecutive winding

sets are imposed. Therefore, the restriction in terms of symmetrical or asymmetrical configurations concerns the single winding set.

Fig. 1 shows two configurations of multiphase windings, facilitating an understanding of the modularity concept. It is noted how a 15-phase symmetrical winding [29] can be configured as *i*) quintuple-three-phase, consisting of five three-phase winding sets (a_k-b_k-c_k, $k = 1 \div 5$) that operate in parallel. In this case, a so-called multi-three-phase machine is obtained [1], which is rather attractive to the industry since the conventional three-phase technologies can be used, reducing cost and design time [4]. However, a 15-phase symmetrical winding can also be configured as *ii*) triple-five-phase, changing the number of neutral points from five to three. In this case, the machine is configured as three five-phase winding sets (a_k-b_k-c_k-d_k-e_k, $k = 1 \div 3$) operating in parallel, allowing for each the use of all fault-tolerant control algorithms developed in the literature [12]–[14], [16], [25], [27].

A. MS Modeling - Modular Application of VSD Approach

According to the MS modeling [1], [31], for each winding set k ($k = 1 \div n$), a dedicated VSD transformation is applied [29], highlighting the k-set torque production. Based on the literature [16], the VSD approach performs a harmonic decoupling action, thus decomposing the k-set model (phase-coordinates) in (l-g)/2 orthogonal subspaces plus g zero-sequence components [29]. In detail, if the number of phases l of each winding set is odd, then $g = 1$. If l is even, and the winding sets have a symmetrical configuration, then $g = 2$. Finally, if l is even, and the winding sets have an asymmetrical configuration, then $g = 0$ since no zero-sequence components exist [29].

The energy conversion is performed in the main stationary subspace (αβ), parallel to those defined for the other sets. Therefore, the (αβ) model of each winding set can be computed in the rotating (dq) coordinates, using the well-known rotational transformation [5]. Like the three-phase machines, the d-axis position ϑ_r is assumed to coincide with the PM flux linkage vector. In summary, for each winding set k ($k = 1 \div n$), the application of the VSD- and rotational- transformations leads to the following (dq) model:

$$\begin{cases} \bar{v}_{sk,dq} = R_s \cdot \bar{i}_{sk,dq} + \dfrac{d}{dt}\bar{\lambda}_{sk,dq} + J \cdot \omega_r \cdot \bar{\lambda}_{sk,dq} \\ \bar{\lambda}_{sk,dq} = L_{\sigma s} \cdot \bar{i}_{sk,dq} + \begin{bmatrix} M_d & 0 \\ 0 & M_q \end{bmatrix} \cdot \sum_{z=1}^{n} \bar{i}_{sz,dq} + \begin{bmatrix} \lambda_m \\ 0 \end{bmatrix} \end{cases} \quad (1)$$

where $\bar{c}_{sk,dq} = [c_{sk,d}\ c_{sk,q}]^t$ is a generic (dq) vector that can have the meaning of k-set voltage v, k-set current i, or k-set flux linkage λ. The synchronous speed ω_r is computed as $\omega_r = p \cdot \omega_m$, where ω_m is the rotor mechanical speed, and p is the pole pair number. The magnetizing inductances along with the d- and q-axes are denoted with M_d and M_q, respectively, while the amplitude of the PM flux linkage vector is denoted with λ_m. Finally, the variable J represents the matrix definition of the complex vector operator.

It is noted how the modular application of the VSD approach leads to the well-known MS magnetic couplings among the sets [1], [33]–[35], [38]. However, the modular approach emphasizes the k-set torque contribution T_k as:

$$T_k = (l/2) \cdot p \cdot \left(\bar{\lambda}_{sk,dq} \wedge \bar{i}_{sk,dq}\right) \quad (2)$$

where ∧ stands for the operator of outer product. According to [16], the electromagnetic model of each k-set harmonic subspace h ($h = 1 \div (l\text{-}g)/2\text{-}1$), defined in its own stationary coordinates (xy-h), is computed as:

$$\bar{v}_{sk,xy-h} = R_s \cdot \bar{i}_{sk,xy-h} + L_{\sigma s} \cdot \frac{d}{dt}\bar{i}_{sk,xy-h} \quad (3)$$

where $\bar{c}_{sk,xy\text{-}h} = [c_{sk,x\text{-}h}\ c_{sk,y\text{-}h}]^t$ is a generic (xy-h) vector that can have the meaning of k-set voltage v and k-set current i. The harmonic currents do not contribute to energy production. Indeed, based on the literature, their active control is implemented if power-sharing [17], [18], or fault-tolerant-strategies among the k-set phases are in use [25]–[28], [30]. Finally, if the zero-sequence components 0-o exist ($o = 1 \div g$), the related electromagnetic equation is computed as:

$$v_{sk,0-o} = R_s \cdot i_{sk,0-o} + L_{\sigma s} \cdot \frac{d}{dt} i_{sk,0-o} \quad (4)$$

where $v_{sk,0\text{-}o}$ and $i_{sk,0\text{-}o}$ are the 0-o components of voltage and current, respectively. However, since each winding set has an isolated neutral point, the zero-sequence currents are null.

The equivalent steady-state circuit of the machine using the MS approach is shown in Fig. 2. It is noted how the modular application of the VSD transformation leads to a single (dq) circuit, coupling all winding sets of the machine. Conversely, each harmonic subspace, as well as zero-sequence component, has its own and decoupled circuit. Therefore, the MS model allows a double decoupling action of the machine's time-harmonic models: *i*) decoupling among the phases belonging to the same winding set, and *ii*) decoupling among the harmonic subspaces belonging to different winding sets. This feature is proof of how the MS approach allows the implementation of the well-known fault-tolerant strategies reported in the literature [25]–[28], [30]. The only difference is related to how such

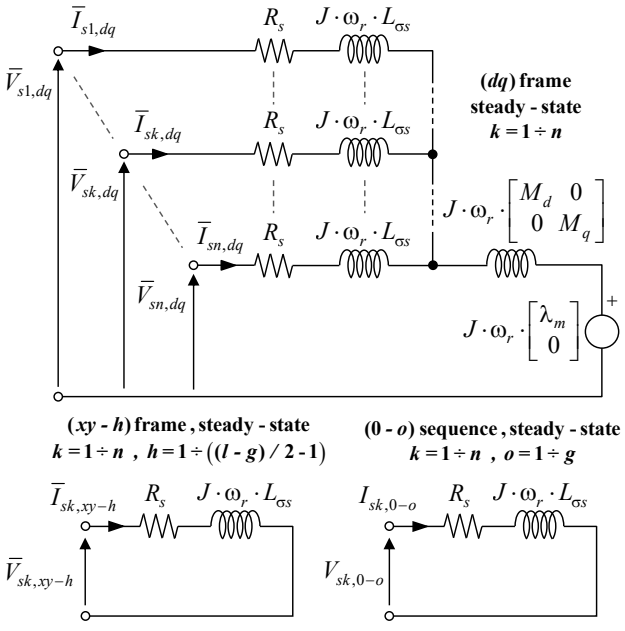

Fig. 2. Steady-state equivalent MS circuit of a multi-l-phase PMSM.

strategies are implemented. They are applied globally to the machine in the VSD-based control schemes, while they are applied to each winding set modularly in the MS-based ones, reducing the complexity.

B. Global Application of the VSD Approach

The VSD model of a PMSM machine is available in the literature [6], [38]. In the following, the main results of such an approach are reported, showing the differences with respect to MS modeling.

It is highlighted again that the VSD approach can be applied globally to the machine only if the stator winding has a symmetrical or asymmetrical configuration [29]. In this case, the torque production is performed in a single (*dq*) subspace, representing the time-fundamental model of the machine, whose electromagnetic equations are:

$$\begin{cases} \bar{v}_{s,dq} = R_s \cdot \bar{i}_{s,dq} + \dfrac{d}{dt}\bar{\lambda}_{s,dq} + J \cdot \omega_r \cdot \bar{\lambda}_{s,dq} \\ \bar{\lambda}_{s,dq} = L_{\sigma s} \cdot \bar{i}_{s,dq} + \begin{bmatrix} n \cdot M_d & 0 \\ 0 & n \cdot M_q \end{bmatrix} \cdot \bar{i}_{s,dq} + \begin{bmatrix} \lambda_m \\ 0 \end{bmatrix} \end{cases} \tag{5}$$

It is noted how (5) is similar to the *k*-set MS model (1). However, in this case, the (*dq*) vectors are representative of all stator phases, leading to an average machine model. It is noted how the couplings among the sets have been removed. However, the modularity is lost. Indeed, (5) is associated with the total machine torque *T*, since this is computed as:

$$T = \sum_{k=1}^{n} T_k = \left(\frac{n \cdot l}{2}\right) \cdot p \cdot \left(\bar{\lambda}_{s,dq} \wedge \bar{i}_{s,dq}\right) \tag{6}$$

The application of the VSD transformation to the whole machine model leads to (n·(l-g)/2-1) harmonic subspaces and (n·g) zero-sequence components, where g is defined as for the MS modeling [29]. Both the harmonic and zero-sequence components are representative of all phases because:

$$\begin{cases} \bar{v}_{s,xy-h} = R_s \cdot \bar{i}_{s,xy-h} + L_{\sigma s} \cdot \dfrac{d}{dt}\bar{i}_{s,xy-h} \\ v_{s,0-o} = R_s \cdot i_{s,0-o} + L_{\sigma s} \cdot \dfrac{d}{dt} i_{s,0-o} \end{cases} \tag{7}$$

where $h = 1 \div (n \cdot (l\text{-}g)/2\text{-}1)$ and $o = 1 \div (n \cdot g)$. Therefore, the global application of the VSD transformation leads to the steady-state circuit of the machine shown in Fig. 3. It is noted how the (*dq*) circuit corresponds to that defined for the three-phase PMSMs, making the VSD modeling the simplest approach to describe the overall torque production. Finally, the equivalent circuits of the harmonic and zero-sequence components are formally identical to those defined for the MS modeling (Fig. 2), leading to similar considerations.

C. Decoupled MS Modeling

The proposed modeling approach aims to remove the MS couplings among the sets, thus introducing a new reference transformation. In detail, the devised method consists of decomposing the (*dq*) models of the sets (1) in multiple decoupled subspaces, having the meaning of common and differential modes of the machine. The torque production is performed in the common-mode subspace, whose equations are identical to those of the VSD modeling (5)-(6), while the unbalances among the sets in terms of flux linkage and torque production are mapped in the differential-mode subspaces.

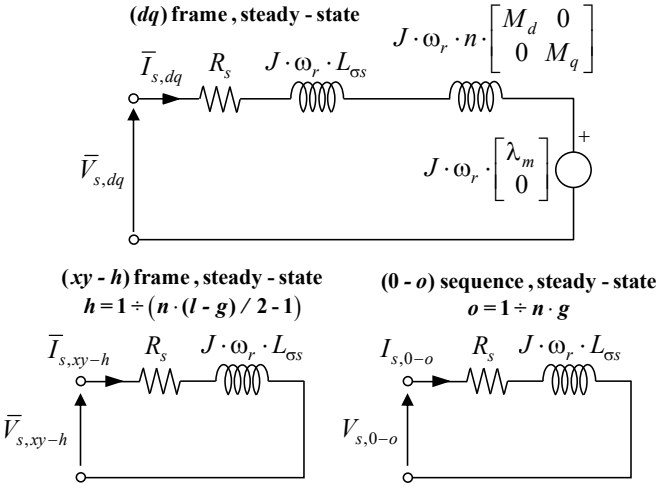

Fig. 3. Steady-state equivalent VSD circuit of a multi-*l*-phase PMSM.

All the current-to-flux relationships of the MS modeling are considered (1), thus merging the (*dq*) components of the sets in a single vector:

$$\begin{bmatrix} \bar{\lambda}_{s1,dq} \\ \bar{\lambda}_{s2,dq} \\ \dots \\ \bar{\lambda}_{sn,dq} \end{bmatrix} = L_{\sigma s} \cdot \begin{bmatrix} \bar{i}_{s1,dq} \\ \bar{i}_{s2,dq} \\ \dots \\ \bar{i}_{sn,dq} \end{bmatrix} + \left[M_{dq}\right] \cdot \begin{bmatrix} \bar{i}_{s1,dq} \\ \bar{i}_{s2,dq} \\ \dots \\ \bar{i}_{sn,dq} \end{bmatrix} + \begin{bmatrix} \bar{\lambda}_{m,dq} \\ \bar{\lambda}_{m,dq} \\ \dots \\ \bar{\lambda}_{m,dq} \end{bmatrix} \tag{8}$$

where $\bar{\lambda}_{m,dq} = [\lambda_m \; 0]^t$ while $[M_{dq}]$ is a ($2n \times 2n$) matrix defined as:

$$\left[M_{dq}\right] = \begin{bmatrix} M_d & 0 & \dots & \dots & M_d & 0 \\ 0 & M_q & \dots & \dots & 0 & M_q \\ \dots & \dots & \dots & \dots & \dots & \dots \\ \dots & \dots & \dots & \dots & \dots & \dots \\ M_d & 0 & \dots & \dots & M_d & 0 \\ 0 & M_q & \dots & \dots & 0 & M_q \end{bmatrix} \tag{9}$$

The removal of the MS couplings consists of diagonalizing the magnetizing inductance matrix (9).

In this paper, the following decoupling transformation is proposed:

$$\begin{bmatrix} \bar{c}_{scm,dq} \\ \bar{c}_{sdm-1,dq} \\ \dots \\ \bar{c}_{sdm-(n-1),dq} \end{bmatrix} = \left[D\right] \cdot \begin{bmatrix} \bar{c}_{s1,dq} \\ \bar{c}_{s2,dq} \\ \dots \\ \bar{c}_{sn,dq} \end{bmatrix} \tag{10}$$

It is noted how the generic MS variable $\bar{c}_{sk,dq}$ (v,i,λ) is expressed as a linear combination of one common-mode vector $\bar{c}_{scm,dq}$ and (n-1) differential-mode vectors $\bar{c}_{sdm\text{-}u,dq}$ (u=1÷(n-1)), using the following ($2n \times 2n$) decoupling matrix:

$$[D]=\frac{1}{n}\cdot\begin{bmatrix} I_{2\times2} & I_{2\times2} & I_{2\times2} & I_{2\times2} & \dots \\ Y_1 & -X_1 & -X_1 & -X_1 & \dots \\ 0_{2\times2} & Y_2 & -X_2 & -X_2 & \dots \\ 0_{2\times2} & 0_{2\times2} & Y_3 & -X_3 & \dots \\ \dots & \dots & \dots & \dots & \dots \\ 0_{2\times2} & 0_{2\times2} & 0_{2\times2} & 0_{2\times2} & \dots \\ 0_{2\times2} & 0_{2\times2} & 0_{2\times2} & 0_{2\times2} & \dots \end{bmatrix} \begin{bmatrix} \dots & I_{2\times2} & I_{2\times2} & I_{2\times2} & I_{2\times2} \\ \dots & -X_1 & -X_1 & -X_1 & -X_1 \\ \dots & -X_2 & -X_2 & -X_2 & -X_2 \\ \dots & -X_3 & -X_3 & -X_3 & -X_3 \\ \dots & \dots & \dots & \dots & \dots \\ \dots & 0_{2\times2} & Y_{n-2} & -X_{n-2} & -X_{n-2} \\ \dots & 0_{2\times2} & 0_{2\times2} & Y_{n-1} & X_{n-1} \end{bmatrix} \tag{11}$$

where $I_{2\times2}$ is a (2×2) identity matrix, $0_{2\times2}$ is a (2×2) zero matrix, while the submatrices X_u and Y_u (u=1÷(n-1)) are defined as:

$$Y_u=(n-u)\cdot X_u \ , \ X_u=x_u\cdot I_{2\times2} \tag{12}$$

The decoupling coefficient x_u (u=1÷(n-1)) must guarantee the removal of the MS couplings, leading to the following definition:

$$x_u=\sqrt{n\Big/\left[(n-u)^2+(n-u)\right]} \tag{13}$$

The decoupling transformation has the amplitude-invariant propriety, and it can be inverted easily since $[D]^{-1}=n\cdot[D]^t$. The matrix coefficients depend only on the number of winding sets n, regardless of the number of phases l composing them. Indeed, by considering three winding sets (n=3), the decoupling matrix is computed as:

$$[D]_{n=3}=\frac{1}{3}\cdot\begin{bmatrix} 1 & 0 & 1 & 0 & 1 & 0 \\ 0 & 1 & 0 & 1 & 0 & 1 \\ \sqrt{2} & 0 & -1/\sqrt{2} & 0 & -1/\sqrt{2} & 0 \\ 0 & \sqrt{2} & 0 & -1/\sqrt{2} & 0 & -1/\sqrt{2} \\ 0 & 0 & \sqrt{3/2} & 0 & -\sqrt{3/2} & 0 \\ 0 & 0 & 0 & \sqrt{3/2} & 0 & -\sqrt{3/2} \end{bmatrix} \tag{14}$$

Such a matrix (14) can be used to decouple any triple-l-phase configuration, e.g., a triple-three-phase (9-phase) or a triple-five-phase (15-phase, Fig. 1), thus showing a high level of versatility. Finally, it is noted how the proposed decoupling matrix is sparse, facilitating its implementation in commercial microcontrollers. By applying (10), (11) to (8), the magnetic (dq) model is computed as:

$$\begin{cases} \bar{\lambda}_{scm,dq}=L_{\sigma s}\cdot\bar{i}_{scm,dq}+\begin{bmatrix} n\cdot M_d & 0 \\ 0 & n\cdot M_q \end{bmatrix}\cdot\bar{i}_{scm,dq}+\begin{bmatrix}\lambda_m\\0\end{bmatrix} \\ \bar{\lambda}_{sdm-u,dq}=L_{\sigma s}\cdot\bar{i}_{sdm-u,dq} \end{cases} \tag{15}$$

where (u=1÷(n-1)). Therefore, all the MS couplings have been removed, leading to a magnetic model that is formally identical to that obtained with the VSD approach (5). However, by applying the decoupling transformation to the voltage (dq) equations of the MS modeling (1), the following is obtained:

$$\begin{cases} \bar{v}_{scm,dq}=R_s\cdot\bar{i}_{scm,dq}+\dfrac{d}{dt}\bar{\lambda}_{scm,dq}+J\cdot\omega_r\cdot\bar{\lambda}_{scm,dq} \\ \bar{v}_{sdm-u,dq}=R_s\cdot\bar{i}_{sdm-u,dq}+\dfrac{d}{dt}\bar{\lambda}_{sdm-u,dq}+J\cdot\omega_r\cdot\bar{\lambda}_{sdm-u,dq} \end{cases} \tag{16}$$

It is noted how, compared to the VSD harmonic subspaces (7), those of differential modes are characterized by the motional voltage terms. Finally, the torque-production is performed in the common-mode subspace, whose physical meaning is identical to that of the (dq) VSD subspace. Indeed, the machine's torque is computed as:

$$T=\sum_{k=1}^{n}T_k=\left(\frac{n\cdot l}{2}\right)\cdot p\cdot\left(\bar{\lambda}_{scm,dq}\wedge\bar{i}_{scm,dq}\right) \tag{17}$$

Therefore, the steady-state equivalent circuit of the machine using the new modeling approach is the same as that depicted in Fig. 2. However, the (dq) circuit containing all MS couplings is replaced with that shown in Fig. 4.

In summary, the proposed decoupling transformation allows getting a decoupled multi-stator (DMS) modeling, extending the results obtained in [40], [41]. In those works, the decoupling transformation can decouple a dual-three-phase PMSM, giving results similar to those obtained in this paper using (11) by considering two l-phase winding sets (n = 2).

D. Comparison between DMS and VSD Approaches

DMS modeling leads to a machine model (15)-(17) similar to that obtained with the VSD approach (5)-(7). However, the meaning of such models is different from each other. The VSD modeling subspaces represent all machine phases, and they are computed using a harmonic decoupling approach [15], [29]. A generic time-harmonic variable (v,i,λ) is mapped only in a single subspace, allowing its control using a pair of regulators (e.g., resonant controllers [17], [43]). The power-sharing strategies among the phases, including the fault-tolerant operation, are performed through the active control of the harmonic subspaces [17], [25], [27]. Therefore, for each winding configuration, it is necessary to identify the harmonic subspaces that perform the desired action. As an example, a 9-phase machine (symmetrical or asymmetrical) using a triple-three-phase configuration is considered.

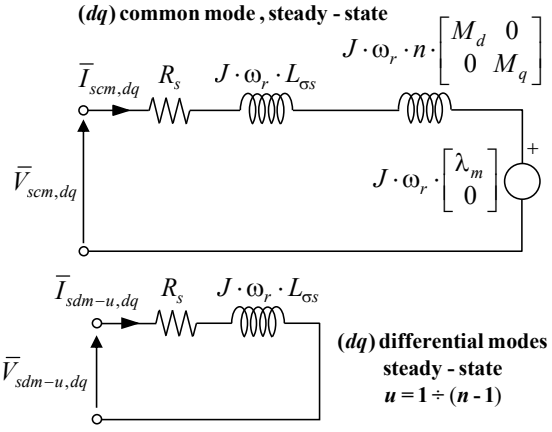

Fig. 4. Steady-state equivalent DMS circuit of a multi-l-phase PMSM.

Based on [17], starting from the (*dq*) currents of the winding sets (MS modeling), the currents of VSD subspaces are computed as:

$$\begin{cases} \overline{i}_{s,dq} = (1/3)\cdot\left(\overline{i}_{s1,dq} + \overline{i}_{s2,dq} + \overline{i}_{s3,dq}\right) \\ i_{s,d-1} = (1/6)\cdot\left[\left(2\cdot i_{s1,d} - i_{s2,d} - i_{s3,d}\right) + \sqrt{3}\cdot\left(i_{s2,q} - i_{s3,q}\right)\right] \\ i_{s,q-1} = (1/6)\cdot\left[\sqrt{3}\cdot\left(i_{s2,d} - i_{s3,d}\right) - \left(2\cdot i_{s1,q} - i_{s2,q} - i_{s3,q}\right)\right] \\ i_{s,d-2} = (1/6)\cdot\left[\left(2\cdot i_{s1,d} - i_{s2,d} - i_{s3,d}\right) - \sqrt{3}\cdot\left(i_{s2,q} - i_{s3,q}\right)\right] \\ i_{s,q-2} = (1/6)\cdot\left[\sqrt{3}\cdot\left(i_{s2,d} - i_{s3,d}\right) + \left(2\cdot i_{s1,q} - i_{s2,q} - i_{s3,q}\right)\right] \end{cases} \quad (18)$$

where it is noted how the harmonic variables (7) are expressed in (*dq*) coordinates, thus applying the rotational transformation on the direct-sequence harmonic subspaces and the inverse rotational transformation on the inverse-sequence ones. In this way, in steady-state conditions, the harmonic variables become dc quantities, allowing their control with conventional proportional-integral (PI) regulators. It can be noted how the (*dq*) currents of the harmonic subspaces are computed as linear combinations of the (*dq*) currents of the winding sets, although there is cross-coupling among the (*dq*) axes.

Compared to the VSD approach, the DMS modeling performs the power-sharing among the phases of each winding set using the harmonic subspaces related to it (3), while the power-sharing among the winding sets is performed using the common- and differential-mode subspaces (10). Indeed, considering the previous example, the currents of such subspaces are computed as:

$$\begin{cases} \overline{i}_{scm,dq} = (1/3)\cdot\left(\overline{i}_{s1,dq} + \overline{i}_{s2,dq} + \overline{i}_{s3,dq}\right) \\ \overline{i}_{sdm-1,dq} = \left(\sqrt{2}/6\right)\cdot\left(2\cdot\overline{i}_{s1,dq} - \overline{i}_{s2,dq} - \overline{i}_{s3,dq}\right) \\ \overline{i}_{sdm-2,dq} = \left(1/\sqrt{6}\right)\cdot\left(\overline{i}_{s2,dq} - \overline{i}_{s3,dq}\right) \end{cases} \quad (19)$$

It can be seen how no cross-coupling among the (*dq*) axes exists, allowing the vector notation also for the differential-mode subspaces. Besides, such equations are valid for all triple-*l*-phase configurations, regardless of the phases number *l* of each winding set ($l \geq 3$), thus providing general validity. Conversely, (18) is valid only for the 9-phase machine using a triple-three-phase configuration and only if the stator winding is symmetrical or asymmetrical. Otherwise, the VSD approach would not even be applicable.

Therefore, the VSD solutions require the computation of the relationships between the harmonic subspaces representing all phases ($n \cdot l$) and the (*dq*) currents belonging to each specific winding set (*l*-phases). For $l = 3$, corresponding to the multi-three-phase configurations [1], [4] the general VSD solutions are provided in [17]. However, in that work, the currents of the harmonic subspaces are computed in stationary coordinates. Indeed, the computation of the (*dq*) VSD solutions requires the knowledge of each harmonic subspace sequence, making a detailed analysis of each multiphase winding configuration necessary. Conversely, the DMS modeling is highly general since the common- and differential-mode variables are defined directly as linear combinations of the winding sets' (*dq*) currents (10)-(11). For this reason, the modularity is fully preserved, and the obtained solutions are not dependent on the phase number *l* of the winding sets.

Regardless of the considered control approach (VSD, MS, or DMS), the power-sharing strategies lead to a reduction of the machine efficiency. Indeed, only the winding sets' balanced operation can minimize the overall Joule losses [17]. However, with the development of the "series/parallel configurations" [17], [44], [45], the control solutions able to perform the power-sharing among the winding sets have gained more attention, leading to several technical contributions [17], [18], [32], [36], [37]. Also, for testing high-power machines, the power-sharing strategies are a viable solution for performing back-to-back regenerative tests [37], [46], [47], thus avoiding the need for expensive high-power prime movers.

Finally, it should be emphasized that the DMS approach does not guarantee the same proprieties as the VSD in terms of harmonic decoupling. Harmonic mapping (as harmonic order, all shown with unity amplitudes) in stationary coordinates, for an asymmetrical 9-phase machine, configured as a triple-three-phase one, is shown in Figs. 5 and 6, to facilitate the understanding. Time-harmonics up to the 31st order have been considered, as after the 17th harmonic and its multiples, the pattern is repeated [29]. Since the VSD main subspace (αβ) and DMS common-mode one have the same meaning, the same time-harmonics map into them. Similarly, identical mapping results are obtained for the zero-sequence components.

However, different mapping results are obtained if one compares the VSD harmonic subspaces with the DMS differential ones. The VSD modeling maps each time-harmonic in a single subspace (see Fig. 5), allowing its control using only a pair of resonant regulators [17], [43]. Therefore, in a non-sinusoidal PMSM, this approach is the most suitable one for performing the torque enhancement using the harmonics above the time-fundamental [48]. With regard to the DMS differential-mode subspaces, it is noted how the same time-harmonics map into them (see Fig. 6), making necessary use of two pairs of resonant regulators in the considered case and *n*-1 in a generic one to perform the control of each time-harmonic.

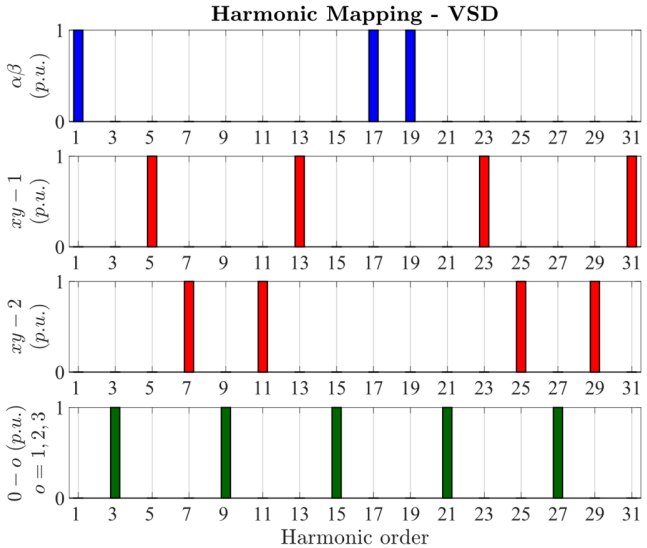

Fig. 5. Harmonic mapping of an asymmetrical 9-phase machine using VSD.

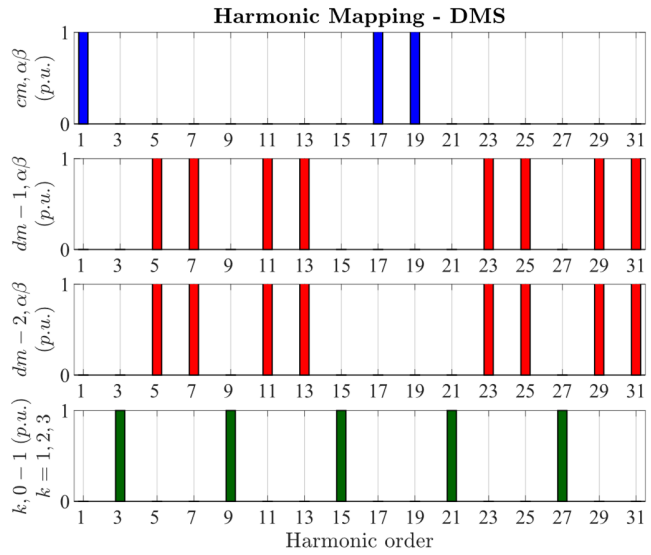

Fig. 6. Harmonic mapping of an asymmetrical 9-phase machine using DMS.

As a summary, for the cases in which the VSD modeling can be applied (symmetrical or asymmetrical windings), the DMS approach represents a competitive alternative for performing the time-fundamental torque control of the PMSM, thus providing the advantages stated in Section I.

III. Modular and Decoupled CVC Scheme

The proposed control solution allows CVC implementation for a generic PMSM with a modular configuration of the stator winding, thus presenting general validity. In detail, the new decoupling transformation (11) is implemented to the basic structure of an MS-based CVC scheme [32], [34], [36]. Therefore, for each generic winding set k (k=1÷n), a dedicated CVC is implemented, thus confirming the proposed control solution's modularity. In the following, the superscripts * and $\tilde{}$ denote a reference and an estimated variable, respectively.

A. Modular CVC

The (dq) current references $\bar{\imath}^*_{sk,dq}$ of the generic set k (k=1÷n) are computed using the torque-to-currents relationships of the machine, as shown in Fig. 7. Therefore, an optimal control strategy can consist of using the maximum-torque per ampere (MTPA) profiles [49], minimizing the k-set phase-currents' amplitude for each k-set reference torque T_k^* value. Although the evaluation of the MTPA profiles usually requires accurate machine mapping [50], the optimal (dq) reference currents can be computed easily if a non-saturated surface-mount PMSM is considered:

$$i^*_{sk,d} = 0 \;,\; i^*_{sk,q} = \left(2/l\right)\cdot T_k^* \Big/ \left(p\cdot\tilde{\lambda}_m\right) \qquad \forall k = 1\div n \qquad (20)$$

The computation of the (dq) reference currents for other PMSM typologies, as well as the evaluation of the torque-to-currents relationships in flux-weakening operation, are not considered here since they are beyond the scope of this paper.

The references of the k-set (xy-h) currents $\bar{\imath}^*_{sk,xy-h}$ (h=1÷(l-g)/2-1) are usually set to zero if the winding set k operates in normal conditions. However, if an open-phase fault occurs, all the fault-tolerant algorithms developed in the literature can be implemented [14], [25]–[28].

Indeed, the harmonic VSD subspaces of each winding set are fully decoupled from those of the others (3). For example, a triple-five-phase PMSM is considered (Fig.1). In this case (n=3, l=5), for each winding set, the fault-tolerant strategies that have been defined for the five-phase machine [25], [27], [28] can be implemented, thus demonstrating how the proposed solution allows using most of the remarkable know-how reported in the literature.

Finally, the k-set (αβ) and (xy-h) feedback currents are computed by applying the VSD transformation [29] to the measured k-set phase-currents [$i_{sk,a\div...}$]; while the k-set (dq) currents are obtained by applying the rotational transformation [5] to the stationary (αβ) components.

B. Decoupled CVC using the DMS-approach

The control of the winding sets' (dq) currents is performed using the DMS approach, thus removing all the couplings related to the modular application of the VSD transformation. Therefore, using the new decoupling transformation (11), both the reference and feedback (dq) currents are computed into their equivalent common- and differential-mode variables, as shown in Fig. 8. In this way, the machine torque is regulated through the CVC of the common-mode subspace. In parallel, the torque unbalances among the winding sets are managed through the CVC of the (n-1) differential-mode subspaces.

In steady-state conditions, common- and differential-mode variables are dc quantities (10), allowing their control using conventional PI controllers. Such regulator's design is simple

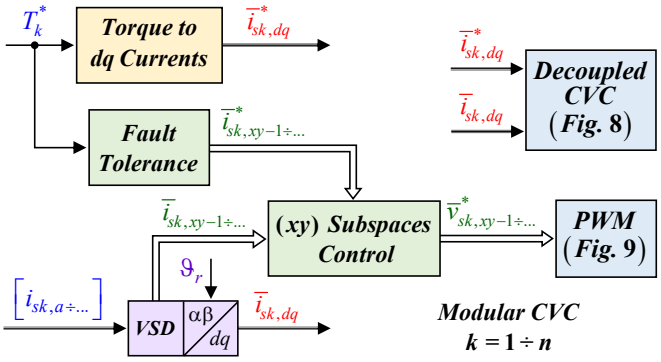

Fig. 7. Modular CVC scheme for a generic multiple-l-phase PMSM.

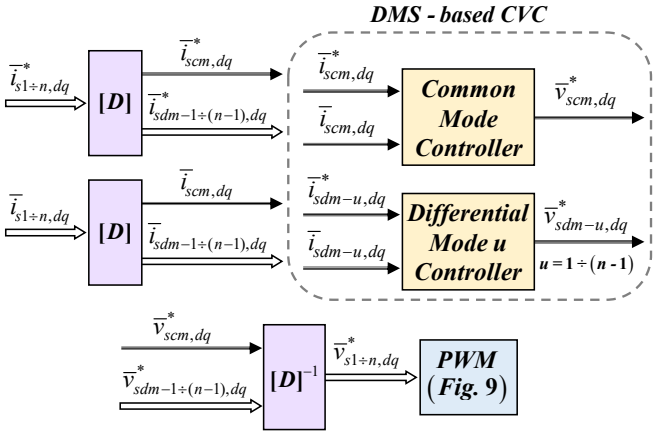

Fig. 8. DMS-based CVC scheme of a generic multiple-l-phase PMSM.

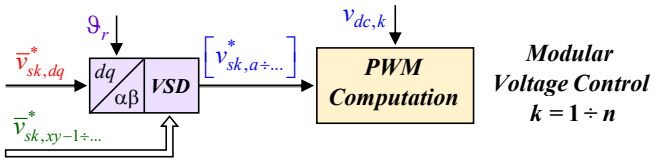

Fig. 9. Modular voltage control of a generic multiple-*l*-phase PMSM.

since the (*dq*) equations of the common-mode subspace (15)-(16) are formally identical to those of a three-phase PMSM, allowing the adoption of the well-known tuning procedures. Besides, the PI controllers dealing with the differential-mode variables are even easier to design since the related equations (15)-(16) correspond to those of a resistor-inductor circuit (R_s-$L_{\sigma s}$) with simple back-emf voltages.

The PI controllers' outputs correspond to the common- and differential-mode reference voltages. Therefore, by applying the inverse of the decoupling transformation (11), the (*dq*) reference voltages of the sets are computed (Fig. 8).

C. Modular Voltage Control

The *k*-set reference voltages in stationary coordinates (αβ) are computed by applying the inverse rotational transformation on the *k*-set (*dq*) reference voltages, as shown in Fig. 9. The (αβ) components are thus merged with the *k*-set reference voltages of the VSD harmonic subspaces $\bar{v}^*_{sk,xy-h}$ (h=1÷(*l*-*g*)/2-1). In this way, the inverse VSD transformation to compute the *k*-set reference phase-voltages $[v^*_{sk,a\div...}]$ is applied. Finally, based on the dc-link voltage $v_{dc,k}$ of the *l*-phase VSI feeding the winding set *k*, the latter's PWM voltage control is performed.

It is noted that the PWM voltage control of each winding set is decoupled from those of the others due to modularity. Therefore, the voltage control of each *l*-phase winding set can be performed using the PWM algorithms reported in the literature [19], regardless of whether SV [20]–[22] or CB [23], [24] approaches are implemented. In summary, as for the fault-tolerant control strategies, the proposed control solution allows using most of the know-how reported in the literature for the standard multiphase configurations.

IV. Experimental Validation

The validation of the DMS approach and the developed CVC scheme has been carried out on a 9-phase surface-mount PMSM using a triple-three-phase configuration (n=3, l=3). The machine has been obtained from a 3-phase PMSM with 6 poles and 36 slots, allowing the use of the off-the-shelf stator cores to reduce cost and design time [51].

However, due to the high number of rotor poles and stator phases, the overall number of slots has not been sufficient to make a symmetrical or asymmetrical winding configuration [29]. As a result, the spatial displacement between the first phases of two consecutive sets is 15 electrical degrees instead of the conventional values of either 20 or 40 electrical degrees [29], as shown in Fig. 10. Therefore, the global application of the VSD modeling has not been possible, making the DMS approach a viable control solution together with the conventional MS-based CVC scheme [32], [34], [36].

Besides, due to several asymmetries of the stator winding, set 2 is characterized by different resistance and leakage inductance values. However, such imbalances among the sets' parameters have allowed the validation of the proposed control solution as the torque regulation is not affected by them. Indeed, just a negligible coupling among the common- and differential-modes subspaces arises, thus further demonstrating the proposed control solution's robustness. In Table I, the machine's primary parameters are listed [34], [36].

A. Test Rig

The PMSM under test has been mounted on a test rig for validation purposes. The rotor shaft has been coupled to a dc machine acting as a prime mover (Fig. 11). The rotor mechanical position has been measured with an incremental encoder with a resolution of 1000 pulses/r. Due to the test rig's mechanical limitations, the machine speed has been limited at ±1500 r/min.

The power converter consists of three custom-made VSIs, based on the insulated-gate bipolar transistor modules (Infineon FS50R12KE3, 50 A, 1200 V). The VSIs are fed by a bidirectional dc power source at 450 V. The switching frequency has been set at 5 kHz, with a hardware-implemented dead-time of 6 µs. The PWM voltage control of each VSI has

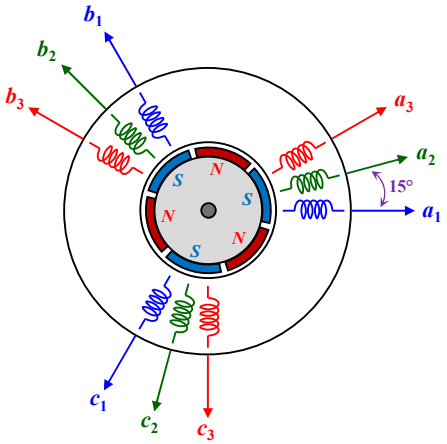

Fig. 10. Nine-phase surface-mount PMSM using a triple three-phase configuration of the stator winding (6 poles).

TABLE I
Parameters of the PMSM under test

Symbol	Parameter	Unit	Value
$n{\cdot}l$	number of phases	-	9 (n=3, l=3)
p	pole pairs	-	3
T_{rated}	rated torque	N·m	7.1
P_{rated}	rated power	kW	1.1
R_s	stator resistance	Ω	8.2 (Set 1 & Set 3) 7.9 (Set 2)
$L_{\sigma s}$	stator leakage inductance	mH	18.5 (Set 1 & Set 3) 10.3 (Set 2)
M_d, M_q	magnetizing inductances	mH	10.5
λ_m	PM flux linkage	V·s	0.265
I_{rated}	rated RMS current	A	1.4
J_{eq}	mechanical inertia	kg·m^2	0.0133

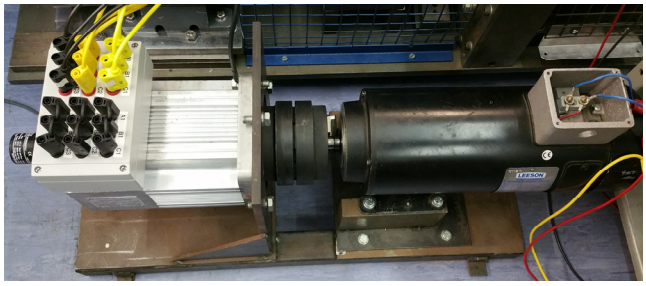

Fig. 11. View of the PMSM under test (left) and driving machine (right).

been performed using the 'MinMax' modulation [52], thus using a CB approach. Finally, the digital controller consists of the dSPACE DS1006 Processor Board, using 10 kHz of sampling frequency (double-edge PWM modulation).

B. Experimental Results

The experimental results are provided for torque control mode. Since the machine under test is a surface-mount PMSM, the reference (*dq*) currents of the winding sets have been computed using the torque-to-current relationships reported in (20). Besides, since the machine stator consists of three winding sets, the decoupling transformation has been computed by setting n =3, as shown in (14). The torque produced by each winding set k (k = 1,2,3) has been estimated using (20) as:

$$\tilde{T}_k = (3/2)\cdot p\cdot \tilde{\lambda}_m \cdot i_{sk,q} \tag{21}$$

Finally, according to (6), the overall machine torque T has been estimated as the sum of the winding sets' torque contributions.

Experimental results are provided for the following tests:

1) Torque step response with three active sets;
2) Torque step response with two active sets;
3) Torque-sharing capability;
4) Fault ride-through capability.

The amplitude limit of the phase-currents has been set at 3.5 A for all winding sets, allowing an overload torque of 175 % (12.4 Nm) of the rated value T_{rated} (7.1 Nm).

1) Torque step response with three active sets: the dc machine has been turned off, emulating an inertial load. The balanced operation of the winding sets has been imposed. The torque has been controlled using a 2-level hysteresis mechanism (±12.4 Nm), keeping the machine speed within the test rig limits (±1500 r/min). After having crossed the zero-speed threshold three times, the VSIs have been turned OFF. The obtained test results are shown in Figs. 12 – 14. Since the PMSM under test has been operated in healthy conditions keeping the winding sets' torque contributions identical, only the common-mode subspace has been actively controlled (see Fig. 12). Therefore, such results are similar to those obtained with a VSD-based control scheme operating in the same conditions. The only difference is related to the VSD harmonic subspaces that are replaced with the differential-mode ones.

Concerning the differential-mode (*dq*) currents, a small interaction between the subspaces is noted due to the imbalance of the winding sets' stator parameters. However, neither uncontrolled overshoots nor steady-state error of the torque regulation has been reported.

The torque regulation modularity is shown in Fig. 13, providing the time-evolution of the winding set torque contributions and (*dq*) currents during the test. Although such variables have not been directly controlled, it is noted how their responses are typical of the MS-based CVC scheme [32], [36], proving how the proposed solution can combine the advantages of both VSD and MS modeling approaches.

To summarise, through this test, the torque regulation's high dynamic performance in healthy conditions has been demonstrated, as further proved in Fig. 14, showing how the machine phase-currents are controlled to their maximum amplitude limit (3.5 A) without any problems.

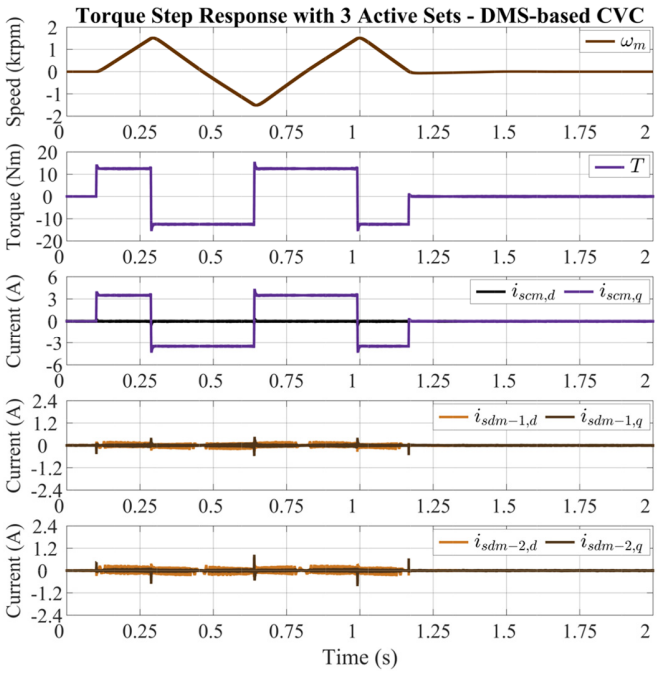

Fig. 12. Torque steps response with three active sets: DMS-based CVC.

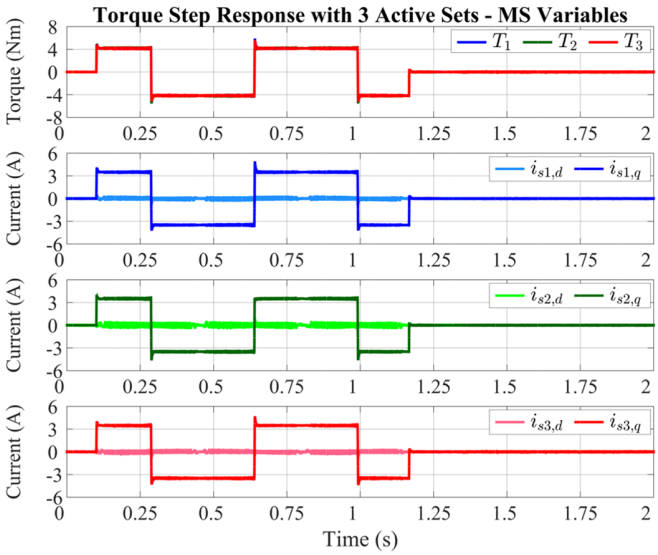

Fig. 13. Torque steps response with three active sets: MS variables.

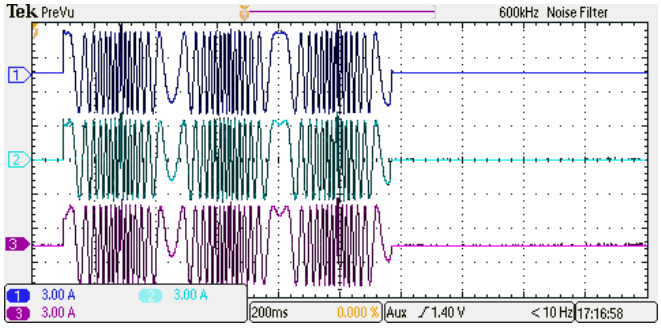

Fig. 14. Torque steps response with three active sets: phase-currents. Ch1: $i_{s1,a}$ (3A/div), Ch2: $i_{s2,a}$ (3A/div), Ch3: $i_{s3,a}$ (3A/div). Time scale: 200 ms/div.

2) Torque step response with two active sets: the previous test has been repeated by controlling the torque of the set 3 to zero. In this case, the machine's torque limit corresponds to two-thirds of the maximum value (8.27 Nm). The obtained test results are shown in Figs. 15–17. It is noted how this test has required more time to be performed (about 0.5 s more), as the maximum acceleration has decreased from 9000 to 6000 r/min/s due to the reduction of the maximum torque limit.

Compared to the previous test, Fig. 15 shows how the differential-modes (*dq*) currents have been actively controlled. Indeed, since the torque contribution of the set 3 is missing, an imbalance among the sets has occurred. Most of the considerations made for the previous test are still valid. Indeed, it is noted how the torque contributions of the active sets and the related *q*-axis current components have a time-evolution that is typical of an MS-based CVC scheme (Fig. 16). However, no complex decoupling algorithms have been implemented, in contrast to [34], [36], as the new transformation (14) allows performing a torque regulation similar to that of a VSD-based CVC scheme. The main difference is related to the fact that

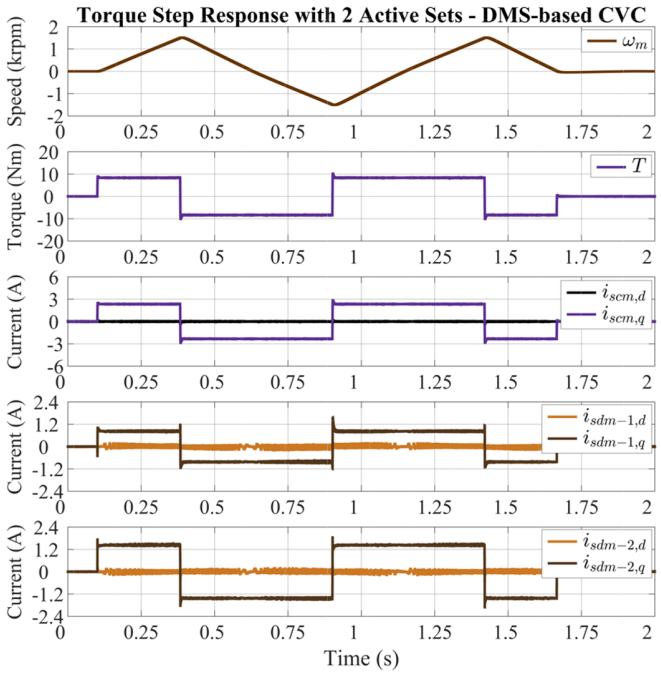

Fig. 15. Torque steps response with two active sets: DMS-based CVC.

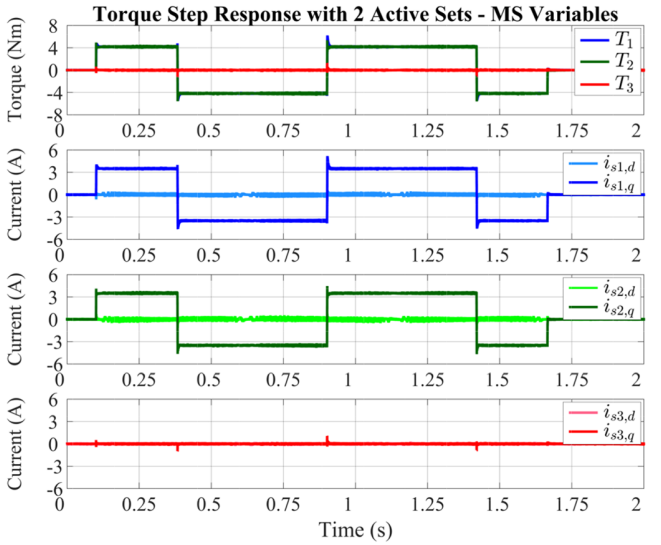

Fig. 16. Torque steps response with two active sets: MS variables.

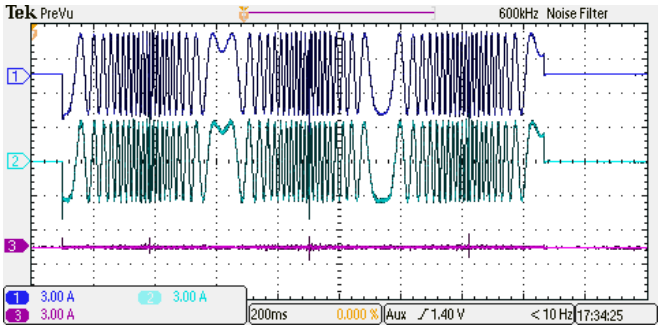

Fig. 17. Torque steps response with two active sets: phase-currents. Ch1: $i_{s1,a}$ (3A/div), Ch2: $i_{s2,a}$ (3A/div), Ch3: $i_{s3,a}$ (3A/div). Time scale: 200 ms/div.

the VSD harmonic subspaces are usually controlled in stationary coordinates, leading to the control of time-fundamental current components. Conversely, the differential mode variables are dc quantities in steady-state conditions, and, as such, they can be controlled using standard PI regulators.

3) Torque-sharing capability: the torque-sharing operation has been tested at 1500 r/min imposed by the dc machine (speed-controlled) and with a constant PMSM torque of 6 Nm. Initially, such a condition has been performed by imposing the winding sets' balanced operation, corresponding to setting of a reference torque of 2 Nm for each of them. After 0.2 s, the overall torque of 6 Nm has been obtained by setting the reference torque of two winding sets at 4 Nm each, with -2 Nm setting (generation mode) for the third one. The winding set operating in the generation mode has been changed cyclically every 0.4 s as follows: set 1 from 0.2 to 0.6 s, set 2 from 0.6 to 1 s, and set 3 from 1 to 1.4 s. After 1.4 s, the balanced operation of the winding sets has been restored. The obtained results are shown in Figs. 18 – 21.

It is noted how only the differential-mode subspaces have been actively regulated (see Fig. 18), as the *q*-axis common-mode current has been controlled at a constant value of about 1.5 A. Therefore, it is demonstrated how the differential-mode subspaces only aim at managing the imbalance between the

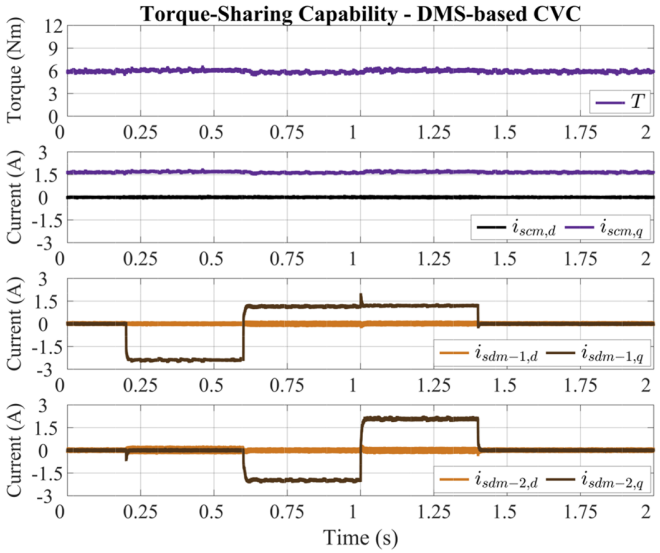

Fig. 18. Torque-sharing capability: DMS-based CVC.

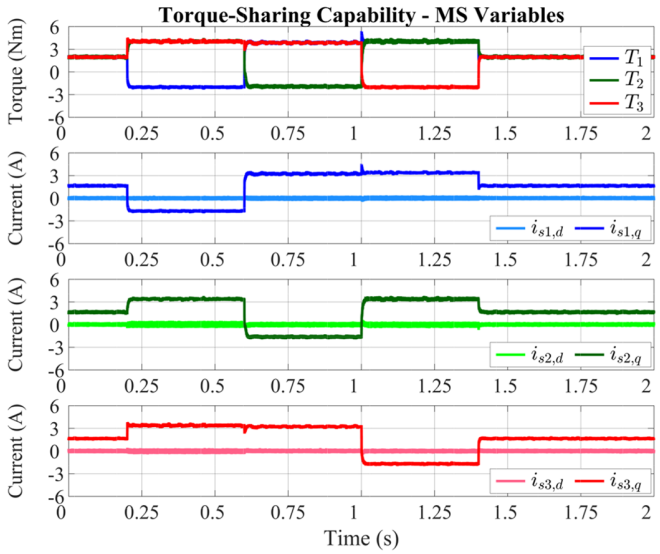

Fig. 19. Torque-sharing capability: MS variables.

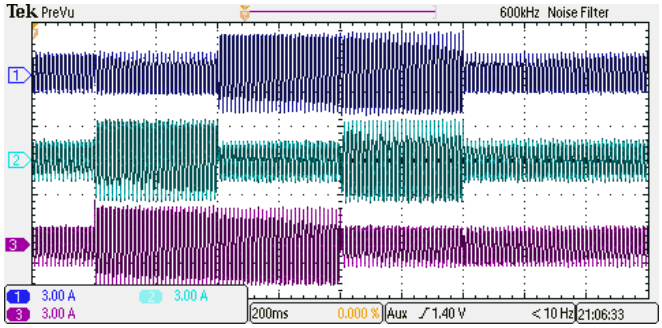

Fig. 20. Torque-sharing capability: phase-currents. Ch1: $i_{s1,a}$ (3A/div), Ch2: $i_{s2,a}$ (3A/div), Ch3: $i_{s3,a}$ (3A/div). Time scale: 200 ms/div.

winding sets in terms of torque, fluxes, or currents. Although this test does not directly relate to any potential practical application, it has fully demonstrated the proposed control solution's torque-sharing capability (see Figs. 19 and 20).

Finally, Fig. 21 shows how the phase-currents of the winding set operating in the generation mode are practically out of phase

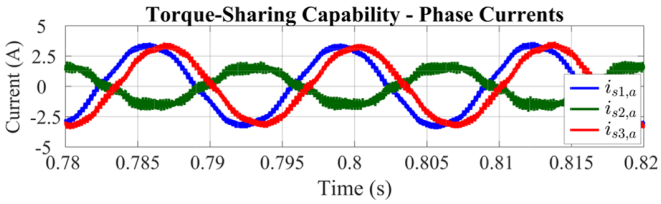

Fig. 21. Torque-sharing capability: zoomed extract from Fig. 20.

with those belonging to the other sets (taking into account the phase shift related to the winding sets' propagation angle, i.e., 15 electrical degrees).

4) Fault ride-through capability: the mechanical speed has been kept at 1500 r/min using the dc machine as a prime mover and with a constant PMSM torque of 8 Nm. The winding sets' balanced operation has been initially imposed, corresponding to set a reference torque of about 2.66 Nm for each of them. After 0.2 s, one of the three VSI units has been turned off cyclically, thus concentrating the overall torque production on two winding sets. The VSI in OFF has been changed cyclically every 0.4 s using the previous test sequence. After 1.4 s, the balanced operation of the winding sets has been restored. The results are shown in Figs. 22–24.

This test shows two simultaneous operating conditions: *i*) torque capability in faulty condition, demonstrating the fault ride-through capability, and *ii*) overload operation since each winding set has been overloaded by a factor close to 168 % (2.35 Arms) to produce the total torque of 8 Nm (see Fig. 23). Like in the previous test, only the differential-mode (d,q) currents have been actively controlled (see Fig. 22). Indeed, the concentration of the torque production on a single winding set can be considered a specific torque-sharing condition. From Fig. 23, it is noted how each winding set has been able to satisfy the torque request without issues, demonstrating the effectiveness of the proposed control solution in open-winding faulty conditions. Finally, it is pointed out how the machine phase-currents have always been kept within the maximum limit (3.5 A) duringthe transients in which the VSI in OFF has been changed, as confirmed in Fig. 24.

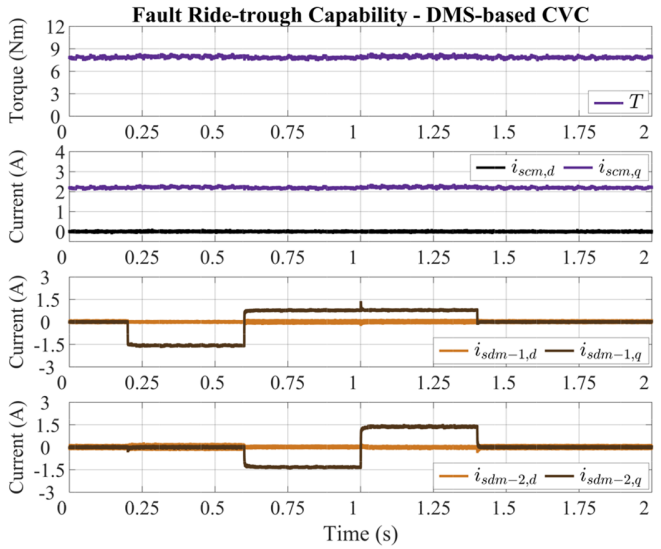

Fig. 22. Fault ride-through capability: DMS-based CVC.

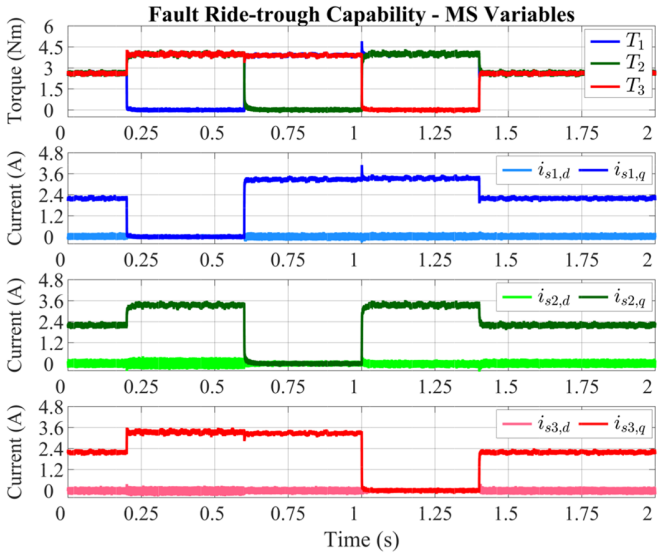

Fig. 23. Fault ride-through capability: MS variables.

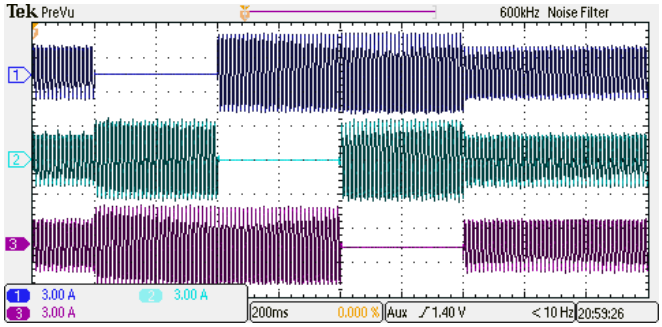

Fig. 24. Fault ride-through capability: phase-currents. Ch1: $i_{s1,a}$ (3A/div), Ch2: $i_{s2,a}$ (3A/div), Ch3: $i_{s3,a}$ (3A/div). Time scale: 200 ms/div.

IV. Conclusion

The paper proposed a new modeling approach for multiphase permanent magnet machines (PMSMs) having a modular configuration of the stator winding. The solution combines the advantages of the vector space decomposition (VSD) and multi-stator (MS) modeling approaches, leading to a modular and decoupled machine model.

The devised modeling approach uses a new decoupling transformation to remove the MS couplings of a generic modular configuration. It is well suited to control of a machine in which unequal power/torque sharing is desirable (as the case may be in future electric vehicles with multiple electric energy sources or microgrids with interconnection through a wind generator), as well as to the control of machines with the non-standard stator winding structure, which is neither symmetrical nor asymmetrical. The novel decoupling transformation has been implemented on the basic structure of the MS-based current vector control (CVC) scheme, leading to a modular and decoupled torque control of a modular multiphase PMSM.

The validation of the developed solution has been carried out with a nine-phase prototype using a triple-three-phase configuration of the stator winding. The experimental results demonstrate the feasibility of the proposed CVC scheme both in regular and faulty operation (modular open-winding faults), as well as the power-sharing capability among the machine's winding sets.

References

[1] R. Bojoi, S. Rubino, A. Tenconi, and S. Vaschetto, 'Multiphase electrical machines and drives: A viable solution for energy generation and transportation electrification', in *2016 International Conference and Exposition on Electrical and Power Engineering (EPE)*, Oct. 2016, pp. 632–639, doi: 10.1109/ICEPE.2016.7781416.

[2] A. Salem and M. Narimani, 'A Review on Multiphase Drives for Automotive Traction Applications', *IEEE Trans. Transp. Electrification*, vol. 5, no. 4, pp. 1329–1348, Dec. 2019, doi: 10.1109/TTE.2019.2956355.

[3] E. Jung, H. Yoo, S. Sul, H. Choi, and Y. Choi, 'A Nine-Phase Permanent-Magnet Motor Drive System for an Ultrahigh-Speed Elevator', *IEEE Trans. Ind. Appl.*, vol. 48, no. 3, pp. 987–995, May 2012, doi: 10.1109/TIA.2012.2190472.

[4] W. Cao, B. C. Mecrow, G. J. Atkinson, J. W. Bennett, and D. J. Atkinson, 'Overview of Electric Motor Technologies Used for More Electric Aircraft (MEA)', *IEEE Trans. Ind. Electron.*, vol. 59, no. 9, pp. 3523–3531, Sep. 2012, doi: 10.1109/TIE.2011.2165453.

[5] P. Krause, O. Wasynczuk, S. D. Sudhoff, and S. Pekarek, *Analysis of Electric Machinery and Drive Systems*. John Wiley & Sons, 2013.

[6] L. Parsa and H. A. Toliyat, 'Five-phase permanent-magnet motor drives', *IEEE Trans. Ind. Appl.*, vol. 41, no. 1, pp. 30–37, Jan. 2005, doi: 10.1109/TIA.2004.841021.

[7] H. Guzman, M. J. Duran, F. Barrero, B. Bogado, and S. Toral, 'Speed Control of Five-Phase Induction Motors With Integrated Open-Phase Fault Operation Using Model-Based Predictive Current Control Techniques', *IEEE Trans. Ind. Electron.*, vol. 61, no. 9, pp. 4474–4484, Sep. 2014, doi: 10.1109/TIE.2013.2289882.

[8] Z. Sun, J. Wang, G. W. Jewell, and D. Howe, 'Enhanced Optimal Torque Control of Fault-Tolerant PM Machine Under Flux-Weakening Operation', *IEEE Trans. Ind. Electron.*, vol. 57, no. 1, pp. 344–353, Jan. 2010, doi: 10.1109/TIE.2009.2029517.

[9] R. Kianinezhad, B. Nahid-Mobarakeh, L. Baghli, F. Betin, and G. Capolino, 'Modeling and Control of Six-Phase Symmetrical Induction Machine Under Fault Condition Due to Open Phases', *IEEE Trans. Ind. Electron.*, vol. 55, no. 5, pp. 1966–1977, May 2008, doi: 10.1109/TIE.2008.918479.

[10] R. Bojoi, M. Lazzari, F. Profumo, and A. Tenconi, 'Digital field-oriented control for dual three-phase induction motor drives', *IEEE Trans. Ind. Appl.*, vol. 39, no. 3, pp. 752–760, May 2003, doi: 10.1109/TIA.2003.811790.

[11] Y. Hu, Z. Zhu, and K. Liu, 'Current Control for Dual Three-Phase Permanent Magnet Synchronous Motors Accounting for Current Unbalance and Harmonics', *IEEE J. Emerg. Sel. Top. Power Electron.*, vol. 2, no. 2, pp. 272–284, Jun. 2014, doi: 10.1109/JESTPE.2014.2299240.

[12] E. Levi, 'Multiphase Electric Machines for Variable-Speed Applications', *IEEE Trans. Ind. Electron.*, vol. 55, no. 5, pp. 1893–1909, May 2008, doi: 10.1109/TIE.2008.918488.

[13] F. Barrero and M. J. Duran, 'Recent Advances in the Design, Modeling, and Control of Multiphase Machines—Part I', *IEEE Trans. Ind. Electron.*, vol. 63, no. 1, pp. 449–458, Jan. 2016, doi: 10.1109/TIE.2015.2447733.

[14] M. J. Duran and F. Barrero, 'Recent Advances in the Design, Modeling, and Control of Multiphase Machines—Part II', *IEEE Trans. Ind. Electron.*, vol. 63, no. 1, pp. 459–468, Jan. 2016, doi: 10.1109/TIE.2015.2448211.

[15] Y. Zhao and T. A. Lipo, 'Space vector PWM control of dual three-phase induction machine using vector space decomposition', *IEEE Trans. Ind. Appl.*, vol. 31, no. 5, pp. 1100–1109, Sep. 1995, doi: 10.1109/28.464525.

[16] E. Levi, R. Bojoi, F. Profumo, H. A. Toliyat, and S. Williamson, 'Multiphase induction motor drives - a technology status review', *IET Electr. Power Appl.*, vol. 1, no. 4, pp. 489–516, Jul. 2007, doi: 10.1049/iet-epa:20060342.

[17] I. Zoric, M. Jones, and E. Levi, 'Arbitrary Power Sharing Among Three-Phase Winding Sets of Multiphase Machines', *IEEE Trans. Ind. Electron.*, vol. 65, no. 2, pp. 1128–1139, Feb. 2018, doi: 10.1109/TIE.2017.2733468.

[18] G. Sala, M. Mengoni, G. Rizzoli, L. Zarri, and A. Tani, 'Decoupled d–q Axes Current-Sharing Control of Multi-Three-Phase Induction Machines', *IEEE Trans. Ind. Electron.*, vol. 67, no. 9, pp. 7124–7134, Sep. 2020, doi: 10.1109/TIE.2019.2941127.

[19] E. Levi, 'Advances in Converter Control and Innovative Exploitation of Additional Degrees of Freedom for Multiphase Machines', *IEEE Trans. Ind. Electron.*, vol. 63, no. 1, pp. 433–448, Jan. 2016, doi: 10.1109/TIE.2015.2434999.

[20] Ó. Lopez, J. Alvarez, J. Doval-Gandoy, and F. D. Freijedo, 'Multilevel Multiphase Space Vector PWM Algorithm', *IEEE Trans. Ind. Electron.*, vol. 55, no. 5, pp. 1933–1942, May 2008, doi: 10.1109/TIE.2008.918466.

[21] Ó. López *et al.*, 'Space-Vector PWM With Common-Mode Voltage Elimination for Multiphase Drives', *IEEE Trans. Power Electron.*, vol. 31, no. 12, pp. 8151–8161, Dec. 2016, doi: 10.1109/TPEL.2016.2521330.

[22] A. Lega, M. Mengoni, G. Serra, A. Tani, and L. Zarri, 'Space Vector Modulation for Multiphase Inverters Based on a Space Partitioning Algorithm', *IEEE Trans. Ind. Electron.*, vol. 56, no. 10, pp. 4119–4131, Oct. 2009, doi: 10.1109/TIE.2009.2020701.

[23] L. Zarri, M. Mengoni, A. Tani, G. Serra, and D. Casadei, 'Minimization of the Power Losses in IGBT Multiphase Inverters with Carrier-Based Pulsewidth Modulation', *IEEE Trans. Ind. Electron.*, vol. 57, no. 11, pp. 3695–3706, Nov. 2010, doi: 10.1109/TIE.2010.2041737.

[24] Ó. López *et al.*, 'Carrier-Based PWM Equivalent to Multilevel Multiphase Space Vector PWM Techniques', *IEEE Trans. Ind. Electron.*, vol. 67, no. 7, pp. 5220–5231, Jul. 2020, doi: 10.1109/TIE.2019.2934029.

[25] A. Mohammadpour and L. Parsa, 'Global Fault-Tolerant Control Technique for Multiphase Permanent-Magnet Machines', *IEEE Trans. Ind. Appl.*, vol. 51, no. 1, pp. 178–186, Jan. 2015, doi: 10.1109/TIA.2014.2326084.

[26] I. G. Prieto, M. J. Duran, P. Garcia-Entrambasaguas, and M. Bermudez, 'Field-Oriented Control of Multiphase Drives With Passive Fault Tolerance', *IEEE Trans. Ind. Electron.*, vol. 67, no. 9, pp. 7228–7238, Sep. 2020, doi: 10.1109/TIE.2019.2944056.

[27] A. Tani, M. Mengoni, L. Zarri, G. Serra, and D. Casadei, 'Control of Multiphase Induction Motors With an Odd Number of Phases Under Open-Circuit Phase Faults', *IEEE Trans. Power Electron.*, vol. 27, no. 2, pp. 565–577, Feb. 2012, doi: 10.1109/TPEL.2011.2140334.

[28] S. Dwari and L. Parsa, 'An Optimal Control Technique for Multiphase PM Machines Under Open-Circuit Faults', *IEEE Trans. Ind. Electron.*, vol. 55, no. 5, pp. 1988–1995, May 2008, doi: 10.1109/TIE.2008.920643.

[29] I. Zoric, M. Jones, and E. Levi, 'Vector space decomposition algorithm for asymmetrical multiphase machines', in *2017 International Symposium on Power Electronics (Ee)*, Oct. 2017, pp. 1–6, doi: 10.1109/PEE.2017.8171682.

[30] N. K. Nguyen, F. Meinguet, E. Semail, and X. Kestelyn, 'Fault-Tolerant Operation of an Open-End Winding Five-Phase PMSM Drive With Short-Circuit Inverter Fault', *IEEE Trans. Ind. Electron.*, vol. 63, no. 1, pp. 595–605, Jan. 2016, doi: 10.1109/TIE.2014.2386299.

[31] R. H. Nelson and P. C. Krause, 'Induction Machine Analysis for Arbitrary Displacement Between Multiple Winding Sets', *IEEE Trans. Power Appar. Syst.*, vol. PAS-93, no. 3, pp. 841–848, May 1974, doi: 10.1109/TPAS.1974.293983.

[32] A. Galassini, A. Costabeber, M. Degano, C. Gerada, A. Tessarolo, and R. Menis, 'Enhanced Power Sharing Transient With Droop Controllers for Multithree-Phase Synchronous Electrical Machines', *IEEE Trans. Ind. Electron.*, vol. 66, no. 7, pp. 5600–5610, Jul. 2019, doi: 10.1109/TIE.2018.2868029.

[33] S. Rubino, R. Bojoi, F. Mandrile, and E. Armando, 'Modular Stator Flux and Torque Control of Multiphase Induction Motor Drives', in *2019 IEEE International Electric Machines and Drives Conference (IEMDC)*, San Diego, USA, 2019, pp. 531–538, doi: 10.1109/IEMDC.2019.8785376.

[34] S. Rubino, R. Bojoi, E. Levi, and O. Dordevic, 'Vector Control of Multiple Three-Phase Permanent Magnet Motor Drives', in *IECON 2018 - 44th Annual Conference of the IEEE Industrial Electronics Society*, Oct. 2018, pp. 5866–5871, doi: 10.1109/IECON.2018.8591146.

[35] D. Hadiouche, H. Razik, and A. Rezzoug, 'Modelling of a double-star induction motor with an arbitrary shift angle between its three phase windings', in *Proc. Int. Conf. PEMC*, Kosice, Slovakia, 2000, p. 5.125-5.130.

[36] S. Rubino, O. Dordevic, R. Bojoi, and E. Levi, 'Modular Vector Control of Multi-Three-Phase Permanent Magnet Synchronous Motors', *IEEE Trans. Ind. Electron.*, pp. 1–1, 2020, doi: 10.1109/TIE.2020.3026271.

[37] S. Rubino, R. Bojoi, F. Mandrile, and E. Armando, 'Modular Stator Flux and Torque Control of Multi-Three-Phase Induction Motor Drives', *IEEE Trans. Ind. Appl.*, pp. 1–1, 2020, doi: 10.1109/TIA.2020.3022338.

[38] Y. Hu, Z. Q. Zhu, and M. Odavic, 'Comparison of Two-Individual Current Control and Vector Space Decomposition Control for Dual Three-Phase PMSM', *IEEE Trans. Ind. Appl.*, vol. 53, no. 5, pp. 4483–4492, Sep. 2017, doi: 10.1109/TIA.2017.2703682.

[39] M. Zabaleta, E. Levi, and M. Jones, 'Modelling approaches for triple three-phase permanent magnet machines', in *2016 XXII International Conference on Electrical Machines (ICEM)*, Sep. 2016, pp. 466–472, doi: 10.1109/ICELMACH.2016.7732567.

[40] S. Kallio, M. Andriollo, A. Tortella, and J. Karttunen, 'Decoupled d-q Model of Double-Star Interior-Permanent-Magnet Synchronous Machines', *IEEE Trans. Ind. Electron.*, vol. 60, no. 6, pp. 2486–2494, Jun. 2013, doi: 10.1109/TIE.2012.2216241.

[41] J. Karttunen, S. Kallio, P. Peltoniemi, P. Silventoinen, and O. Pyrhönen, 'Decoupled Vector Control Scheme for Dual Three-Phase Permanent Magnet Synchronous Machines', *IEEE Trans. Ind. Electron.*, vol. 61, no. 5, pp. 2185–2196, May 2014, doi: 10.1109/TIE.2013.2270219.

[42] S. Rubino, R. Bojoi, D. Cittanti, and L. Zarri, 'Decoupled and Modular Torque Control of Multi-Three-Phase Induction Motor Drives', *IEEE Trans. Ind. Appl.*, vol. 56, no. 4, pp. 3831–3845, 2020, doi: 10.1109/TIA.2020.2991122.

[43] R. I. Bojoi, G. Griva, V. Bostan, M. Guerriero, F. Farina, and F. Profumo, 'Current control strategy for power conditioners using sinusoidal signal integrators in synchronous reference frame', *IEEE Trans. Power Electron.*, vol. 20, no. 6, pp. 1402–1412, Nov. 2005, doi: 10.1109/TPEL.2005.857558.

[44] M. J. Durán, S. Kouro, B. Wu, E. Levi, F. Barrero, and S. Alepuz, 'Six-phase PMSG wind energy conversion system based on medium-voltage multilevel converter', in *Proceedings of the 2011 14th European Conference on Power Electronics and Applications*, Aug. 2011, pp. 1–10.

[45] I. Zoric, M. Jones, and E. Levi, 'Voltage balancing control of a symmetrical nine-phase machine with series-connected DC links', in *2017 IEEE 26th International Symposium on Industrial Electronics (ISIE)*, Jun. 2017, pp. 1052–1057, doi: 10.1109/ISIE.2017.8001391.

[46] A. A. Abduallah, O. Dordevic, M. Jones, and E. Levi, 'Regenerative Test for Multiple Three-Phase Machines With Even Number of Neutral Points', *IEEE Trans. Ind. Electron.*, vol. 67, no. 3, pp. 1684–1694, Mar. 2020, doi: 10.1109/TIE.2019.2903750.

[47] M. Zabaleta, E. Levi, and M. Jones, 'A Novel Synthetic Loading Method for Multiple Three-Phase Winding Electric Machines', *IEEE Trans. Energy Convers.*, vol. 34, no. 1, pp. 70–78, Mar. 2019, doi: 10.1109/TEC.2018.2850976.

[48] M. Slunjski, O. Stiscia, M. Jones, and E. Levi, 'General Torque Enhancement Approach for a Nine-Phase Surface PMSM with Built-in Fault Tolerance', *IEEE Trans. Ind. Electron.*, pp. 1–1, 2020, doi: 10.1109/TIE.2020.3007053.

[49] T. M. Jahns, G. B. Kliman, and T. W. Neumann, 'Interior Permanent-Magnet Synchronous Motors for Adjustable-Speed Drives', *IEEE Trans. Ind. Appl.*, vol. IA-22, no. 4, pp. 738–747, Jul. 1986, doi: 10.1109/TIA.1986.4504786.

[50] E. Armando, R. I. Bojoi, P. Guglielmi, G. Pellegrino, and M. Pastorelli, 'Experimental Identification of the Magnetic Model of Synchronous Machines', *IEEE Trans. Ind. Appl.*, vol. 49, no. 5, pp. 2116–2125, Sep. 2013, doi: 10.1109/TIA.2013.2258876.

[51] A. S. Abdel-Khalik, A. M. Massoud, and S. Ahmed, 'Application of Standard Three-Phase Stator Frames in Prime Phase Order Multiphase Machine Construction', *IEEE Trans. Ind. Electron.*, vol. 66, no. 4, pp. 2506–2517, Apr. 2019, doi: 10.1109/TIE.2018.2840497.

[52] D. G. Holmes and T. A. Lipo, *Pulse Width Modulation for Power Converters: Principles and Practice*. John Wiley & Sons, 2003.